International Journal of Rotating Machinery 2005:1, 45–52

Analysis of Secondary Flows in Centrifugal Impellers

Klaus Brun
Mechanical and Fluids Engineering Department, Southwest Research Institute, 6220 Culebra Road, San Antonio, TX 78238-5166, USA
Email: klaus.brun@swri.org

Rainer Kurz
Solar Turbines Incorporated, 9330 Sky Park Court, San Diego, CA 92123-5398, USA
Email: kurz_rainer_x@solarturbines.com

Received 12 October 2003

Secondary flows are undesirable in centrifugal compressors as they are a direct cause for flow (head) losses, create nonuniform meridional flow profiles, potentially induce flow separation/stall, and contribute to impeller flow slip; that is, secondary flows negatively affect the compressor performance. A model based on the vorticity equation for a rotating system was developed to determine the streamwise vorticity from the normal and binormal vorticity components (which are known from the meridional flow profile). Using the streamwise vorticity results and the small shear-large disturbance flow method, the onset, direction, and magnitude of circulatory secondary flows in a shrouded centrifugal impeller can be predicted. This model is also used to estimate head losses due to secondary flows in a centrifugal flow impeller. The described method can be employed early in the design process to develop impeller flow shapes that intrinsically reduce secondary flows rather than using disruptive elements such as splitter vanes to accomplish this task.

Keywords and phrases: pumps, compressors, secondary flows, vorticity, circulating flows.

1. INTRODUCTION

Strong circulatory secondary flows (vortex flows) are observed in mixed-flow impellers such as axial/centrifugal pumps, turbines, and compressors. These vortex flows are undesirable as they are responsible for head losses, flow nonuniformity, and slip. To reduce secondary flows and slip, turbomachinery designers often employ flow guiding/disruptive elements such as splitter vanes and other hardware modifications (which themselves negatively affect the efficiency of the machine) rather than focusing on the actual causes and intrinsic physical mechanism that generate vortex secondary flows.

Most modern commercially available three dimensional (3D) computational fluid dynamics codes can predict circulatory secondary flows in rotating machinery with a reasonable accuracy. However, the aim of this work is not to develop another "black-box" flow prediction tool (such as a 3D Navier-Stokes flow solver), but rather to derive a simplified model from the governing equations to study the underlying physics of the secondary vortex flow phenomena. Results from this paper will provide the designer with a more fundamental understanding of how circulatory secondary flows behave and are affected by operational and geometric parameters of the turbomachine.

To limit the topic somewhat, this paper will focus only on prediction of vortex secondary flows in shrouded centrifugal compressors using the streamwise vorticity equation. (In unshrouded centrifugal compressors the viscous influence of the rotating wall/shroud and tip leakage effects complicate the secondary flows such that a simple model based on the vorticity equation is not directly applicable.) As the influence of the density gradient terms within the streamwise vorticity equation will be demonstrated to be negligible, results from this paper are certainly also applicable to centrifugal pumps.

Thus, a model to determine the rotational direction and magnitude of the passage circulatory secondary flows was derived based on the streamwise vorticity equation. The model applies known meridional velocities to the streamwise vorticity equations to determine normal, binormal, and streamwise vorticity, circulatory secondary velocities, and associated head losses. The influence of nondimensional operating parameters (Reynolds number, Rossby number) on vortex secondary flows is also analyzed.

2. BACKGROUND AND REVIEW OF RELEVANT LITERATURE

During the past 50 years a number of researchers have studied the flow fields in mixed-flow turbomachinery employing both analytical and experimental methods. For the sake of brevity only analysis relevant to the secondary flow field and jet/wake effects (as it relates directly to secondary flows) is presented herein.

Eckardt [1] used the laser-2-focus (L2F) method to measure velocities in radially bladed and backward swept impellers with diffusers. Suction side separation and wake flow was observed. More uniform flow was observed in the backswept impeller.

Fister et al. [2] used L2F to measure flow in simulated bends of multistage radial-flow impellers. Results were compared to predictions from a 3D, turbulent, viscous Navier-Stokes code. Reasonable agreement was found between experimental and computational results; however, the Navier-Stokes code failed to predict existing flow separation regions.

Krain [3] used L2F to study the effect of vaned and vaneless diffusers on impeller flow in a centrifugal compressor. Rapid boundary layer growth and wake flow was shown at the midpassage on the blade suction sides. Similarly, Hayami et al. [4] employed an L2F to measure velocities in the inducer of a centrifugal compressor. Also, static pressure measurements were taken at the shroud. Small separation regions were shown near the inducer inlet, while the flow along the blades was mostly stable, except near the shroud.

Hamkins and Flack [5], Flack et al. [6], and Miner et al. [7] used a two-directional Doppler laser velocimeter to measure the flow of a shrouded and unshrouded centrifugal impeller with logarithmic spiral volutes. Measurements were taken in the impeller and the volute. Nonuniform asymmetric flow was shown at impeller off-design conditions, but jet/wake flow was not observed.

Fagan and Fleeter [8] measured the flows in a centrifugal compressor impeller using a laser velocimeter and a shaft encoder. Significant flow changes as compressor stall approached were identified. Hathaway et al. [9] measured velocities in a large low-speed centrifugal fan using a laser velocimeter. Results were favorably compared to five-hole probe and other data. McFarland and Tiederman [10] used a two-directional laser velocimeter to measure flows in an axial turbine stator cascade. Unsteady flow due to the turbine upstream wakes were seen to affect the flow field throughout the stator.

Strong secondary flows were observed in the mixed-flow pump of a torque converter by Gruver et al. [11] and Brun et al. [12]. Comparable secondary flows in other turbomachinery geometries were studied by a number of researchers. For example, Moore [13, 14] used a hot wire probe to determine the secondary flow field in a rotating radial-flow passage and to compare the results to predictions from a potential flow code. Hawthorne [15], Kelleher et al. [16], and Sanz and Flack [17] studied secondary flows in stationary circular and rectangular bends. Ellis [18] experimentally and analytically studied the induced vorticity in a centrifugal compressor. Krain [19], Moore and Moore [20], Eckardt [1], Howard and Lennemann [21], and Brun et al. [12] experimentally determined the secondary flows in mixed-flow centrifugal impellers. Finally, Johnson and Moore [22] determined secondary flow mixing losses in a centrifugal impeller from pressure probes installed in the rotating impeller.

A number of analytical models have been derived for the development of streamwise vorticity and, thus, vortex secondary flows in turbomachines. Wu et al. [23], Smith [24], Hill [25], Horlock and Lakshminarayana [26], and Lakshminarayana and Horlock [27] derived equations for the development of streamwise vorticity in stationary and rotating systems. Analytical solutions of these equations were presented by Hawthorne [15] for stationary bends and rotating radial-flow passages. Later, Johnson [28] solved these equations to predict secondary flows in a rotating bend.

3. VORTEX FLOW THEORY

Secondary flows are always caused by an imbalance between a static pressure field and the kinetic energy in the flow. An example is the well-documented horseshoe vortex, where the incoming boundary layer flow meets a stagnation line which causes a motion of the fluid along the wall, and subsequently the formation of a vortex. The important observation herein is that the strength of the vortex is mostly determined by the starting conditions and the further development of the vortex is determined by the conservation of its angular momentum. In a rotating system the analogy is that the vortex flows are principally generated by the meridional flow field while the centrifugal and Coriolis forces only act to change the vortex vector direction (tilting of the vortex plane).

The meridional flow in centrifugal/mixed flow pumps and compressors is usually highly nonuniform, dominated by significant jet/wake flow with separation regions blocking up to half of the passage through-flow areas. At high Reynolds numbers, the peak meridional velocities are located at the blade hub-pressure sides due to potential flow effects; at low Reynolds numbers, the viscous jet/wake flow causes the flow to separate at the hub and, thus, the peak velocities are seen at the blade tip-pressure side. These through-flow profiles can be accurately predicted using simple jet/wake flow models (for low Reynolds number, low specific speed impellers), empirical models (based on the significant amount of experimental data available in the public domain), or even Euler flow solvers (for high Reynolds number impellers). Once the meridional flow profile is determined, the normal and binormal vorticity can be numerically evaluated and the results are directly applied to the rotating system vorticity equations to calculate the streamwise vorticity. Using simple potential flow solvers and the viscous dissipation function, the passage circulatory (vortex) secondary flow and associated head losses can be estimated, respectively.

4. SECONDARY FLOW MODEL

Streamwise vorticity and, hence, rotating secondary flows will develop whenever a moving fluid with a gradient of the reduced stagnation pressure ($P_{rs} = P + 1/2\rho(V^2 - \omega^2 R^2)$) turns around a bend or is rotated about a fixed axis (Johnson [28]). A gradient in the reduced stagnation pressure, P_{rs}, might result from a nonuniform velocity profile or a reduction of P_{rs} due to boundary layer viscous dissipation. In centrifugal impellers the meridional flow field is highly nonuniform because of the jet/wake flow phenomena, the nonuniform flow field is both turned around a bend with a radius of curvature r, and is rotated around the shaft at an angular speed of ω. Hence, high values of streamwise vorticity and strong associated circulatory secondary flows are anticipated.

Equations for the generation of streamwise vorticity, and, thus, circulatory secondary flows, in an intrinsic rotating coordinate system were first derived by Hawthorne [15], Smith [29], Smith [24], and Ellis [18]. These equations were then generalized to include viscous terms and compressibility effects by Howard [30] and Lakshminarayana and Horlock [27]. The equations as derived by Lakshminarayana and Horlock were employed for the analysis herein.

Since a detailed derivation of these equations is available in the literature, only the main steps for the inviscid, incompressible streamwise vorticity generation equations are described here. The steady-state, incompressible Navier-Stokes equations for a rotating system are given in vector form by

$$(V \cdot \nabla)V = -\nabla\left(\frac{P}{\rho}\right) + \upsilon\nabla^2 V + 2\omega \times V + \omega \times (\omega \times r), \tag{1}$$

where V is the velocity vector, P is the total pressure, υ is the kinematic viscosity, and ω is the angular velocity of the system. One should note that the fourth term in (1) represents the Coriolis force and the fifth term represents the centrifugal force. Also, note that the equations are being derived with the assumption of incompressible flow; the subject analysis found that for the generation of streamwise vorticity in centrifugal compressors, the fluid compressibility effects were found to be negligible (see more detailed explanation below).

Introducing the vector identity,

$$(V \cdot \nabla)V = \frac{1}{2}\nabla(V \cdot V) - V \times (\nabla \times V), \tag{2}$$

defining the vorticity vector, ξ, as

$$\xi = \nabla \times V, \tag{3}$$

and taking the curl of (1) with the knowledge that the curl of a gradient of a scalar always equals zero ($\nabla \times \nabla\Phi = 0$), one obtains

$$\nabla \times (V \times \xi) = \upsilon\nabla^2\xi + 2\nabla \times (\omega \times V). \tag{4}$$

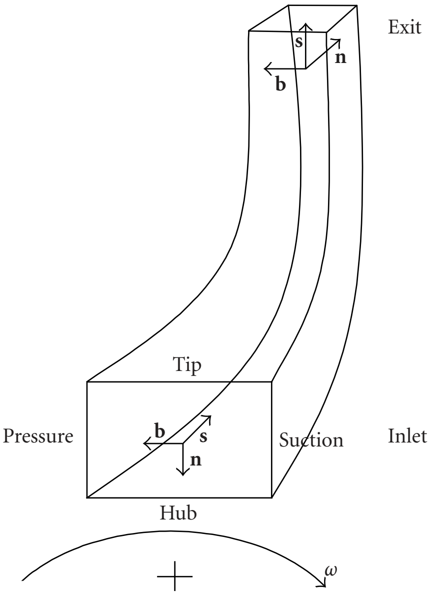

FIGURE 1: Intrinsic coordinate system in centrifugal impeller.

Furthermore, introducing the vector identities,

$$\begin{gathered}\nabla \times (V \times \xi) = V(\nabla \cdot \xi) - \xi(\nabla \cdot V) - (V \cdot \nabla)\xi + (\xi \cdot \nabla)V, \\ \nabla \cdot \xi = \nabla \cdot \nabla \times V = 0,\end{gathered} \tag{5}$$

and knowing that for an incompressible flow from the continuity equation,

$$\nabla \cdot V = 0, \tag{6}$$

one obtains

$$(V \cdot \nabla)\xi = (\xi \cdot \nabla)V - \upsilon\nabla^2\xi - 2\nabla \times (\omega \times V), \tag{7}$$

which is the vorticity transport equation for an incompressible flow in a rotating system (Greenspan [31]).

Unit vectors are now defined along the streamline, **s** (streamwise), in the inward radius of curvature direction, **n** (normal), and along the **b** (binormal) direction, so that **s**, **n**, and **b** form a right-handed set of unit vectors. In a centrifugal compressor these directions approximately correspond to **s**-through-flow direction, **n**-tip-to-hub side direction, and **b**-suction-to-pressure side direction (see Figure 1).

Taking the dot product of (7) (and neglecting the viscous term) with the streamwise unit normal vector, **s**, and using the dot product relations given by Bjørgum [32] for an intrinsic coordinate system, one obtains (Lakshminarayana and Horlock [27])

$$|V|\frac{\partial\xi_s}{\partial s} - |V|\frac{\xi_n}{r} = \xi_s\frac{\partial|V|}{\partial s} + |V|\frac{\xi_n}{r} + 2\omega \cdot \nabla V, \tag{8}$$

where r is the radius of curvature and s is along the streamwise direction. This expression can be simplified to obtain the fundamental generation of streamwise vorticity equation for a rotating system (Lakshminarayana and Horlock [27]),

$$\frac{\partial}{\partial s}\left(\frac{\xi_s}{|V|}\right) = 2\frac{\xi_n}{|V|r} - 2\frac{s\cdot(\omega\times\xi)}{|V|^2}, \tag{9}$$

where ξ is the total vorticity vector, ξ_n is the normal vorticity component, ξ_s is the streamwise vorticity component, and r is the radius of curvature. The first term in (9) is a streamline curvature term and the second is a Coriolis force term. For an impeller with a fixed axis of rotation (such as a centrifugal compressor) this equation can be further reduced to

$$\frac{\partial}{\partial s}\left(\frac{\xi_s}{|V|}\right) = 2\frac{\xi_n}{|V|r} - 2\frac{\omega\xi_b\sin\kappa}{|V|^2}, \tag{10}$$

where κ is the meridional flow angle relative to the axis of rotation and ξ_b is the binormal component of vorticity.

The normal and binormal components of vorticity (ξ_n, ξ_b) in (10) can be directly determined from

$$\xi_n = -\frac{1}{A}\iint(\nabla\times U)\cdot dA = -\frac{1}{A}\iint\left(\frac{\partial v}{\partial z}-\frac{\partial w}{\partial y}\right)dA, \tag{11}$$

$$\xi_b = -\frac{1}{A}\iint(\nabla\times V)\cdot dA = -\frac{1}{A}\iint\left(\frac{\partial u}{\partial z}-\frac{\partial w}{\partial x}\right)dA, \tag{12}$$

where A is the through-flow area. For the purpose of this analysis the term $\partial v/\partial z$ in (11) and the term $\partial u/\partial z$ in (12) can be neglected as they are small compared to the meridional gradients ($\partial w/\partial y$ and $\partial w/\partial x$). Thus,

$$\begin{aligned}\xi_n &= \frac{1}{A}\iint\frac{\partial w}{\partial y}dx\,dy,\\ \xi_b &= \frac{1}{A}\iint\frac{\partial w}{\partial x}dx\,dy.\end{aligned} \tag{13}$$

Values for ξ_n and ξ_b can be calculated from (13) if the meridional flow profile is known by discretizing the equations and numerical integration. Namely, the normal and binormal components of the vorticity can be determined for a known meridional flow profile (from jet/wake models, 2D flow through-flow models, and/or experimental data).

Equation (10) shows that there are primarily two force terms that contribute to the generation of streamwise vorticity in a centrifugal impeller. The first term shows that streamwise vorticity is generated whenever a flow that is nonuniform in the pressure-to-suction direction, and thus, has a normal vorticity component, ξ_n, follows a curved bend with a radius of curvature, r. The second term shows streamwise vorticity generation whenever flow that is nonuniform in the hub-to-tip direction (ξ_b) is rotated around a centerline (shaft). The sine-term indicates that streamwise vorticity is only generated by the second term when a radial-flow component ($\kappa \neq 0^\circ$) exists.

Thus, in a compressor, a pressure-to-suction side nonuniform flow profile only contributes to the first term of (10) while a hub-to-tip side nonuniformity only contributes to the second term of (10). The meridional flow angle in (10) can be closely approximated by $\kappa = \pi s/s_{\text{total}}$ for a circular compressor torus. Consequently, (10) with the normal and binormal vorticities obtained from the simple 2D flow models, can be numerically integrated to calculate the streamwise vorticity in the compressor and, thus, can be used to approximately predict the compressor secondary flow circulation.

One should note that streamwise vorticity can also be generated by compressibility effects and viscosity; analytical terms for these effects can be found in Lakshminarayana and Horlock [27] but were found to be negligible in the analysis presented herein. Namely, compressibility and viscosity have a strong direct influence on the meridional flow field and, thus, on the normal and binormal vorticity components, but only an indirect effect on the streamwise vorticity. The secondary flow field is "shaped" by gradients in the reduced stagnation pressure (Johnson [28]) that are principally determined by the meridional flow field, centrifugal forces, and Coriolis forces. Once the meridional flow field is known, the secondary flow field can be determined neglecting compressibility and viscous effects. A vortex will behave mostly under the influence of its angular momentum vector. Clearly, the viscosity of the fluid leads to a small exchange of momentum between the vortex structure and the surrounding flow field, with the net effect that the radius of the vortex will increase and the core vortex strength will decrease as it travels downstream in the impeller. However, this influence is negligible when compared with the inertia of its angular momentum vector and the effects of centrifugal and Coriolis forces.

To qualitatively assess the secondary vortex velocity vector field from the streamwise vorticity, a modified approach to Hawthorne's [15] small shear/large disturbance method, as described by Lakshminarayana and Horlock [33], is used. In this method the relative displacement of the streamlines (and the center of circulation) is determined using the nondimensional meridional velocity profile (weighted mass flow). The small shear/large disturbance approximation is valid here because in the centrifugal compressor flow turning (bending) and not shear (as in an axial impeller) dominates the action on the working fluid (Howard [30]).

In the small shear/large disturbance method the 2D continuity equation ($\partial u/\partial x + \partial v/\partial y = 0$) with the definition of a stream function, $u = -\partial\psi/\partial y$ and $v = \partial\psi/\partial x$, is used to obtain

$$\nabla^2\psi = \frac{\partial^2\psi}{\partial x^2} + \frac{\partial^2\psi}{\partial y^2} = -\xi_s\cdot\frac{w_{i,j}}{w_{\text{ave}}}\cdot dA_{i,j}, \tag{14}$$

where $w_{i,j}$ is the local plane through-flow velocity, $dA_{i,j}$ is the incremental plane area, and w_{ave} is the average plane through-flow velocity. Equation (14) must be solved for the streamfunction, ψ, with the boundary conditions of $\psi = 0$ on the walls. A solution for this can be obtained analytically in the form of a Fourier series or (14) can simply be solved by an iterative numerical approach. Since in a centrifugal compressor the passage planes are not necessarily a perfectly rectangular domain, the numerical solution is preferred for this case. A central difference discretization was applied to (14) to obtain

$$\begin{aligned}\psi_{i,j}^{(\text{new})} &= \frac{1}{4}\left(\psi_{i,j+1}+\psi_{i,j-1}+\psi_{i+1,j}+\psi_{i-1,j}\right)^{(\text{old})}\\ &\quad -\xi_s\cdot\frac{w_{i,j}}{w_{\text{ave}}}\cdot\Delta A_{i,j}.\end{aligned} \tag{15}$$

This equation was solved for $\psi^{(\text{new})}$ by successive iterations (updating $\psi^{(\text{old})}$ in each step) marching over the entire mathematical domain (plane). The normalized through-flow velocities, $w_{i,j}/w_{\text{average}}$, are obtained from the predicted meridional flow profiles. Convergence (total residual of ψ of less than 0.01) is typically achieved after approximately 2000 iterations (passes) over the domain and a resolution of 100×100 grid points is usually adequate. Once a converged solution is obtained, the passage secondary vortex velocities can be determined from the numerical partial derivatives of the streamfunction ($u=-\partial\psi/\partial y$ and $v=\partial\psi/\partial x$).

5. HEAD LOSSES DUE TO SECONDARY FLOWS

The total flow head in a compressor or pump increases as tangential kinetic energy is transferred into the fluid by the rotating blades. However, due to fluid friction (viscosity) the work input to the machine does not equal the isentropic work out; that is, the efficiency is always less than 100%. Thus, the viscous head loss due to secondary flows is an important parameter to estimate the overall performance of a centrifugal compressor.

Using the streamwise vorticity secondary flow models as described above, an estimate of this loss can be determined from the laminar viscous dissipation of the internal flow. (Note that only head losses due to secondary flows are predicted; other significant head losses due to turbulence, laminar meridional dissipation, and unsteady viscous dissipation are not evaluated. Typically head losses due to secondary flows contribute less than 2% to the total head loss in a centrifugal compressor.)

The laminar viscous dissipation function for incompressible flow (and neglecting all meridional flow terms), Φ_{ls}, is

$$\Phi_{\text{ls}} = 2\mu\left[\left(\frac{\partial u}{\partial x}\right)^2+\left(\frac{\partial v}{\partial y}\right)^2\right]+\mu\left(\frac{\partial u}{\partial y}+\frac{\partial v}{\partial x}\right)^2. \tag{16}$$

By integrating the above laminar dissipation, $\Phi_{\text{laminar secondary}}$, across an entire compressor passage, the total head loss per passage due to secondary flows, $\Delta H_{\text{passage}}$, is determined. The total impeller head loss due to secondary flows, $\Delta H_{\text{secondary}}$, is then calculated by multiplying $\Delta H_{\text{passage}}$ by the number of blade passages in the compressor, N. Thus

$$\Delta H_{\text{secondary}} = N\cdot\int\Phi_{\text{ls}}\,dV. \tag{17}$$

Clearly, the secondary flow head loss is directly related to the streamwise vorticity function and thus also related to the nonuniformity of the meridional profile.

6. NONDIMENSIONAL FORCE PARAMETERS

The Rossby number, $\text{Ro} = V/\omega r$, is a measure of inertial to Coriolis force and is commonly employed for turbomachinery flow analysis. However, as centrifugal forces have a stronger influence than inertial forces on the secondary flows in a rotating machine, a modified Rossby number can be introduced:

$$\text{Ro}_m = \frac{F_{\text{centrifugal}}}{F_{\text{Coriolis}}} = \frac{\omega R}{2V}. \tag{18}$$

Namely, Ro_m is a measure of the relative influence of the centrifugal force (in the outward radial direction) versus the Coriolis force (in the counter-rotational tangential direction).

Brun [34] showed that the modified Rossby affects the pressure-to-suction side meridional (jet/wake) flow profile and the normal vorticity, ξ_n. Consequently, the modified Rossby number should have a strong effect on the first term in the streamwise vorticity generation term in (10). On the other hand, the binormal vorticity—the second term in (10)—is not affected by the modified Rossby number directly. However, during actual compressor operation, the modified Rossby number typically changes with pump speed, ω, and thus indirectly relates the Rossby number to the second term of (10).

The Reynolds number, $\text{Re} = Vr/\nu$, is an indicator of inertial versus viscous forces for a moving fluid. Since the Reynolds number primarily influences the hub-to-tip side meridional flow profile, the streamwise vorticity should mostly affect the second term (rotational Coriolis force term) of (10) while the influence on the first term should be weak.

Interestingly, streamwise vorticity theory thus predicts that vortex secondary flows are primarily related to the modified Rossby number (centrifugal/Coriolis force) via first term of (10) and the Reynolds number (inertial/viscous force) via the second term of (10). One should note that the terms of (10) act in the opposite direction: term one is positive and acts to generate vortex secondary flows circulating in the clockwise direction (seen radial-inward) while term two is negative and acts in the counterclockwise direction. That is, a centrifugal compressor can be designed in which the terms of (10) offset each other and circulatory secondary flow generation is minimized.

7. PREDICTED RESULTS AND COMPARISON WITH EXPERIMENTAL DATA

Using the above model, parametric studies were performed to evaluate the relative influence of the nondimensional operating parameters on the centrifugal compressor streamwise vorticity and subsequent passage vortex secondary flows. Of

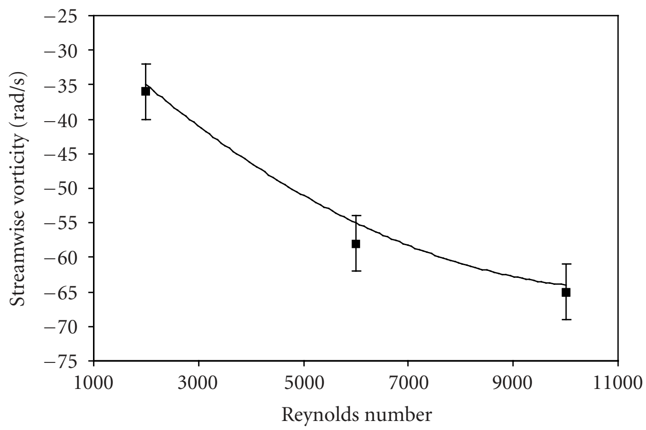

Figure 2: Streamwise vorticity as a function of Reynolds number.

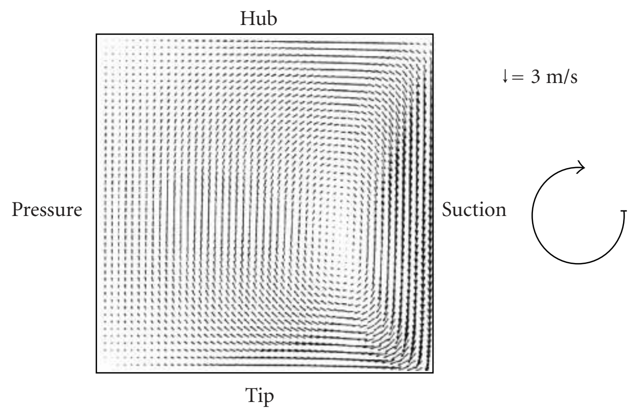

Figure 4: Predicted secondary flow field at impeller exit (Brun [34]).

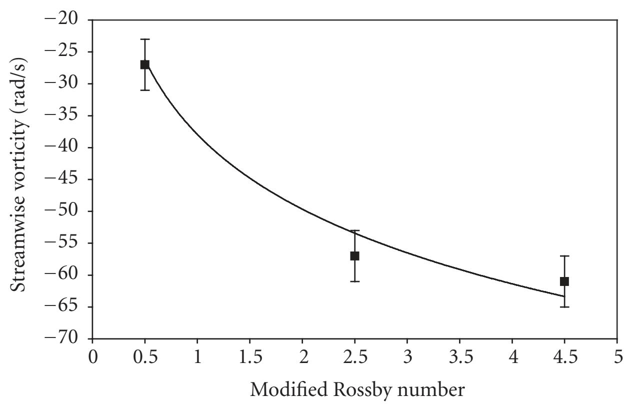

Figure 3: Streamwise vorticity as a function of modified Rossby number.

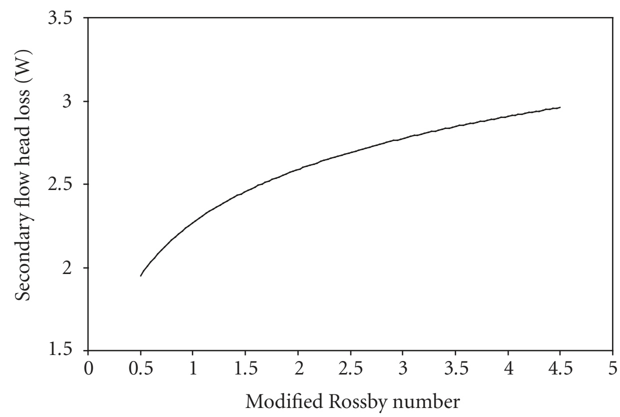

Figure 5: Pump head losses as a function of modified Rossby number.

particular interest is the effect on the flow field of varying the nondimensional force parameters—the Reynolds number and the modified Rossby number—as they represent the changing operating conditions an impeller experiences. For these studies, normal and binormal vorticity results from the pressure-to-suction and hub-to-tip jet/wake flow studies as presented by Brun [34] were used in (10) to determine the streamwise vorticity component. The subject analysis is based on a 30 cm diameter mixed-flow centrifugal impeller geometry, rotating at 1000 rpm with an incompressible, medium viscosity fluid at low Reynolds number operating conditions.

Figures 2 and 3 show predicted streamwise vorticity as a function of Reynolds and modified Rossby numbers. Limited experimental data for a mixed-flow shrouded impeller is shown as a comparison; results are within the uncertainty bands of the flow measurements.

The streamwise vorticity is seen to decrease with Re and Ro_m. Consequently, circulatory secondary flow vectors are expected to increase their clockwise rotation as Re and Ro_m are increased.

Figure 4 shows the predicted secondary velocity field from (15) at 100% span. Clearly, a large circulatory secondary flow vortex, centered at the suction side of the blade, is seen. The secondary flow vortex assumes almost the entire passage width. These results compare favorable to experimental measurements of circulating secondary flows.

Secondary flow head loss trends as a function of modified Rossby number are shown in Figure 5. As a reference, the total head loss for this impeller is approximately 30–40 W. Secondary flow head loss increases with modified Rossby number, which is consistent with the observation that the clockwise circulatory secondary flows increase with modified Rossby number.

8. CONCLUSIONS AND SUMMARY

A model to determine the rotational direction and magnitude of the circulatory velocity in shrouded centrifugal impellers was derived based on the streamwise vorticity governing equation. The model applies known meridional velocities to the streamwise vorticity equations to determine vorticity, circulatory secondary velocities, and associated head losses. Streamwise vorticity, and thus circulatory secondary flow, is seen to be primarily generated by the centrifugal and Coriolis forces on the meridional flow field. Viscous and compressibility effects must be considered to determine the meridional flow field but can be neglected in the streamwise vorticity equations.

A parametric analysis of the generation of streamwise vorticity equation showed that

(i) positive vorticity and, thus, counterclockwise secondary passage flow circulation is generated by the interaction of the pressure-to-suction side meridional flow gradient with the axial-to-radial turning of the flow in the blade passage,

(ii) negative vorticity and, thus, clockwise secondary passage flow circulation is generated by the interaction of the hub-to-tip side meridional flow gradient with the rotation, ω, of the blade passage.

Hence, the nondimensional operational force parameters, modified Rossby number and Reynolds number, directly affected the velocity magnitudes of the vortex secondary flow:

(i) increasing the Reynolds and/or modified Rossby number, Ro_m, increases clockwise flow circulation,

(ii) moderating the pressure-to-suction velocity gradient (e.g., by backsweeping the blades) increases the counterclockwise flow circulation or moderates the clockwise flow circulation.

Comparison with experimental data showed that analytical results from the above streamwise vorticity model are within the uncertainty band of flow measurements in a shrouded mixed-flow impeller; namely, the model can be employed to accurately predict secondary flow trends. The herein described method can be employed early in the design process to optimize impeller flow shapes that intrinsically reduce secondary flows rather than using flow disruptive elements such as splitter to accomplish this task.

REFERENCES

[1] D. Eckardt, "Detailed flow investigations within a high-speed centrifugal compressor impeller," *ASME Journal of Fluids Engineering*, vol. 98, no. 3, pp. 390–402, 1976.

[2] W. Fister, G. Zahn, and F. W. Adrian, "Theoretical and experimental studies of return channels in hydraulic turbomachines," VDI-Berichte, no. 424, pp. 173–192.

[3] H. Krain, "A study on centrifugal impeller and diffuser flow," *ASME Journal of Engineering for Power*, vol. 103, no. 4, pp. 688–697, 1981.

[4] H. Hayami, Y. Senoo, and H. Ueki, "Flow in the inducer of a centrifugal compressor measured with a laser velocimeter," *Journal of Engineering for Gas Turbines and Power*, vol. 107, no. 2, pp. 534–540, 1985.

[5] C. P. Hamkins and R. D. Flack, "Laser velocimeter measurements in shrouded and unshrouded radial flow pump impellers," *ASME Transactions, Journal of Turbomachinery*, vol. 109, no. 1, pp. 70–76, 1987.

[6] R. D. Flack, C. P. Hamkins, and D. R. Brady, "Laser velocimeter turbulence measurements in shrouded and unshrouded radial flow impellers," *International Journal of Heat and Fluid Flow*, vol. 8, no. 1, pp. 16–25, 1987.

[7] S. M. Miner, R. J. Beaudoin, and R. D. Flack, "Laser velocimetry measurements in a centrifugal flow pump," *Journal of Turbomachinery*, vol. 111, no. 3, pp. 205–212, 1989.

[8] J. R. Fagan and S. Fleeter, "Ldv measurements of a mixed-flow impeller at design and near stall," ASME Paper no. 92-GT-310, 1992.

[9] M. D. Hathaway, R. M. Chriss, J. R. Wood, and A. J. Strazisar, "Experimental and computational investigation of the NASA low-speed centrifugal compressor flow field," ASME Paper no. 92-GT-213, 1992.

[10] V. E. McFarland and W. G. Tiederman, "Viscous interaction upstream and downstream of a turbine cascade with a periodic wake field," ASME Paper no. 92-GT-162, 1992.

[11] J. K. Gruver, R. D. Flack, and K. Brun, "Laser velocimeter measurements in the pump of a torque converter, part i - average measurements," *ASME Transactions, Journal of Turbomachinery*, vol. 118, no. 3, pp. 562–569, 1996.

[12] K. Brun, R. D. Flack, and S. B. Ainley, "Secondary flow measurements in a mixed flow pump using laser velocimetry," in *Proc. 7th International Symposium on Applications of Laser Techniques to Fluid Mechanics (ISALT '94)*, Lisbon, Portugal, July 1994.

[13] J. Moore, "A wake and and eddy in a rotating radial-flow passage part 2: Flow model," *ASME Journal of Engineering for Power*, vol. 95, pp. 213–219, 1973.

[14] J. Moore, "A wake and and eddy in a rotating radial-flow passage part 1: Experimental observations," *ASME Journal of Engineering for Power*, vol. 95, pp. 205–212, 1973.

[15] W. R. Hawthorne, "Secondary circulation in fluid flow," in *Proc. Roy. Soo.*, vol. 206, pp. 374–387, London, UK, May 1951.

[16] M. D. Kelleher, D. L. Flentie, and R. J. McKee, "An experimental study of the secondary flow in a curved rectangular channel," *Journal of Fluids Engineering*, vol. 102, pp. 92–96, 1980.

[17] G. M. Sanz and R. D. Flack, "Flow visualization of secondary flows in three curved ducts," ASME Paper no. 86-GT-166, 1986.

[18] G. O. Ellis, "A study of induced vorticity in centrifugal compressors," *ASME Journal of Engineering for Power*, vol. 86, pp. 63–76, 1964.

[19] H. Krain, "Swirling impeller flow," *Journal of Turbomachinery*, vol. 110, pp. 122–128, 1988.

[20] J. Moore and J. G. Moore, "Calculations of three-dimensional viscous flow and wake development in a centrifugal impeller," *ASME Journal of Engineering for Power*, vol. 103, pp. 367–372, 1981.

[21] J. H. G. Howard and E. Lennemann, "Measured and predicted secondary flows in a centrifugal impeller," *ASME Journal of Engineering for Power*, vol. 103, pp. 126–132, 1971.

[22] M. W. Johnson and J. Moore, "Secondary flow mixing losses in a centrifugal impeller," ASME Paper no. 82-GT-44, 1982.

[23] C. H. Wu, C. A. Brown, and V. D. Prian, "An approximate method of determining the subsonic flow in an arbitrary stream filament of revolution cut by arbitrary turbomachine blades," NACA Report no. TN-2702, 1952.

[24] A. G. Smith, "On the generation of the streamwise component of vorticity for flows in rotating passages," *The Aeronautical Quarterly*, pp. 369–382, 1957.

[25] P. G. Hill, "Effects of coriolis on the turbulent boundary layer in rotating fluid machines," MIT, Gas Turbine Laboratory Report, no. 69, 1962.

[26] J. H. Horlock and B. Lakshminarayana, "Secondary flows: theory, experiment and application in turbomachinery aerodynamics," *Ann. Rev. Fluid Mech.*, vol. 5, pp. 247–279, 1973.

[27] B. Lakshminarayan and J. H. Horlock, "Generalized expressions for secondary vorticity using intrinsic co-ordinates," *Journal of Fluid Mechanics*, vol. 59, pp. 97–115, 1973.

[28] M. W. Johnson, "Secondary flow in rotating bends," *ASME Journal of Engineering for Power*, vol. 100, pp. 553–560, 1978.

[29] L. H. Smith, "Secondary flow in axial-flow turbomachinery," *ASME Transactions*, pp. 1065–1076, 1955.

[30] J. H. G. Howard, "Analytical theory of secondary flow in a centrifugal impeller," EIC Report, no. EIC-MECH 4, 1973.

[31] H. P. Greenspan, *The Theory of Rotating Fluids*, Cambridge University Press, Cambridge, Mass, USA, 1968.

[32] O. Bjørgum, "On Beltrami vector fields and flows ($\nabla \times v = \Omega v$). I. A comparative study of some basic types of vector fields," *Univ. Bergen Årbok. Naturvit. Rekke*, vol. 1951, no. 1, pp. 1–86, 1951.

[33] B. Lakshminarayana and J. H. Horlock, "Review: Secondary flows and losses in cascades and axial-flow turbomachines," *International Journal of Mechanical Science*, vol. 5, pp. 287–307, 1963.

[34] K. Brun, *Torque Converter Flow Analysis*, Ph.D. Dissertation, University of Virginia, Charlotesville, Virginia, USA, 1996.